Combining size distribution and chemical species measurements into a multivariate receptor model of $PM_{2.5}$

Timothy V. Larson,[1] David S. Covert,[2] Eugene Kim,[3] Robert Elleman,[2] Astrid B. Schreuder,[4] and Thomas Lumley[5]

Received 28 May 2005; revised 16 September 2005; accepted 4 January 2006; published 10 May 2006.

[1] We introduce an extended receptor model, implemented with the multilinear engine ME2, which combines simultaneous but separate filter-based species information with size-resolved particle volume information. Our chemical data set consisted of 24-hour filter measurements reported by the EPA Speciation Trends Network at Beacon Hill in Seattle, Washington, from February 2000 to June 2003. We measured the particle size distribution at this site from December 2000 to April 2002 using a differential mobility particle sizer (DMPS) and an aerodynamic particle sizer (APS). The combined model extends the traditional chemical mass balance approach by including a simultaneous set of conservation equations for both particle mass and volume, linked by a unique value of apparent particle density for each source. The model distinguished three mobile source features, two consistent with previous identifications of "gasoline" and "diesel" sources, and an additional minor feature enriched in EC, Fe and Mn and ultrafine particle mass that would have been difficult to interpret in the absence of particle size information. This study has also demonstrated the feasibility of defining missing mass as an additional variable, and thereby providing additional useful model constraints and eliminating the posthoc regression step that is traditionally used to rescale the results.

Citation: Larson, T. V., D. S. Covert, E. Kim, R. Elleman, A. B. Schreuder, and T. Lumley (2006), Combining size distribution and chemical species measurements into a multivariate receptor model of $PM_{2.5}$, *J. Geophys. Res.*, *111*, D10S09, doi:10.1029/2005JD006285.

1. Introduction

[2] Multivariate receptor modeling has been widely used to estimate the contribution of various sources to measured airborne particulate matter mass concentrations [*Henry*, 1997; *Hopke*, 1997]. Various algorithms have been used to solve the basic chemical mass balance model to estimate both source contributions and source features, including those implemented in the Unmix [*Henry*, 2003], positive matrix factorization (PMF) [*Paatero*, 1997], and multilinear engine (ME2) [*Paatero*, 1999] computer programs. These algorithms have been mainly applied to chemical species concentrations derived from daily fine particle filter samples. Several investigators have also applied these factor analytic algorithms to size distribution measurements, assuming a unique size distribution for each contributing source and linearity between particle number and mass concentrations over time at a fixed site [*Ruuskanen et al.*, 2001; *Wahlin et al.*, 2001; *Kim et al.*, 2004b; *Zhou et al.*, 2004, 2005].

[3] Recently, Zhou and coworkers [*Zhou et al.*, 2005] have applied PMF to a single data set that includes both chemical species and size-resolved number concentrations. This approach has the advantage of (1) the use of a relatively long time series compared with most studies of particle composition as a function of size that are typically weeks to several months duration [*Phares et al.*, 2003; *Rhoads et al.*, 2003] with only a few studies of longer duration [*Bein et al.*, 2005; *Tolocka et al.*, 2005], (2) precise measures of both species concentrations and particle size, and (3) the potential for widespread application to many locations that have ongoing filter-based measurements by incorporating readily available sizing technology. However, this approach has the disadvantage of (1) not directly measuring the composition of individual particles or particle size fractions, thereby averaging across external mixtures, and (2) averaging over relatively long time periods (e.g., 24 hours), thereby missing important source related variability and making potentially inaccurate assumptions about the stability of source related size features. As size-dependent chemical composition information becomes more widespread and incorporates better time resolution, e.g., via aerosol mass spectrometric analysis, a trilinear mass balance model can be used to provide size-resolved source infor-

[1]Department of Civil and Environmental Engineering, University of Washington, Seattle, Washington, USA.
[2]Department of Atmospheric Sciences, University of Washington, Seattle, Washington, USA.
[3]Department of Civil and Environmental Engineering, Clarkson University, Potsdam, New York, USA.
[4]Department of Environmental and Occupational Health Sciences, University of Washington, Seattle, Washington, USA.
[5]Department of Biostatistics, University of Washington, Seattle, Washington, USA.

Copyright 2006 by the American Geophysical Union.
0148-0227/06/2005JD006285

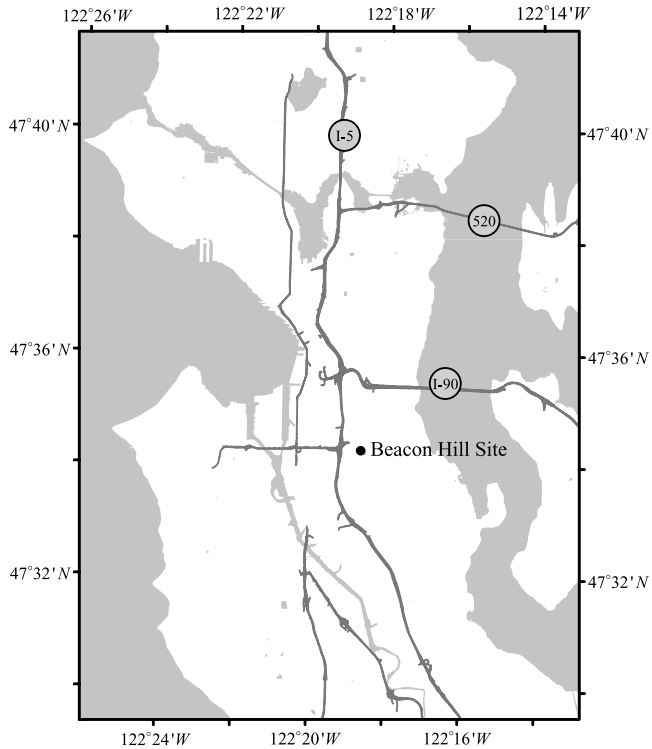

Figure 1. Map of sampling site and surrounding area.

mation. In the interim, we introduce a receptor model that simultaneously balances particle mass and particle volume, implemented with a multivariate receptor model. The model combines 24-hour filter-based species information with size-resolved particle volume information and incorporates a term for unanalyzed or "missing" mass. Because of dynamic nature of particle size distributions in the atmosphere, our main emphasis is still on the filter-based species measurements. Our intent here is to expand the traditional species-based multivariate receptor model by including an ancillary set of size distribution measurements to help inform the basic model. In this way, it is similar to including local meteorological information to help resolve and interpret the extracted features, as has previously been reported [*Paatero and Hopke*, 2003].

2. Methods

2.1. Sampling and Analysis

[4] Our chemical data set consisted of 24-hour filter measurements reported by the EPA Speciation Trends Network at Beacon Hill, Seattle, Washington, from February 2000 to June 2003. Detailed descriptions of the $PM_{2.5}$ measurements [*Kim et al.*, 2005] and quality assurance procedures [*Research Triangle Institute*, 2004] are available. The Beacon Hill site is centrally located within the Seattle urban area; approximately 100 m above sea level (see Figure 1). The hill is part of a larger ridge defining the eastern edge of an area of light industry including a major seaport, an airport and warehousing and trucking activity 1 to 4 km west of the site. Interstate freeways and arterial roads carrying large amounts of traffic are closely situated 2 km northwest of the site. The site is considered to be representative of 24-hour average $PM_{2.5}$ levels within a 20 km radius [*Goswami et al.*, 2002]. The prevailing winds at the monitoring site were from the south (19%), southwest (17%), and northeast (17%). The highest wind speeds (upper 25%) were from the southwest.

[5] We measured the particle number-size distribution at this site from December 2000 to April 2002 using a differential mobility particle sizer (DMPS) and an aerodynamic particle sizer (APS). The DMPS consisted of an electrostatic classifier and a condensation particle counter (models 3081 and 3010, TSI, St. Paul, Minnesota). The DMPS stepped through the mobility size range over a period of 10 min. At the end of each scan sequence, the mobility data were inverted with the charge probability matrix to get the Stokes diameter size distribution in 16 size intervals from 0.020 to 0.6 μm. The size distribution from 0.7 to 5 μm was measured with an APS (model 3310, TSI, St. Paul, Minnesota) on the same 10 min basis to yield the aerodynamic diameter size distribution in 16 intervals. The instrumentation was maintained on a 10 day cycle or as needed during power or other malfunctions. Flow rates, clean air zero tests and instrumental diagnostic parameters were checked and problems noted and corrected as necessary. The relative humidity in the instruments was maintained at less than 30% in the sensing volumes by diffusion drying to establish a consistent reference aerosol state and minimize the effect of hygroscopic growth on the measured time series. The 10 min distributions were edited to eliminate periods of instrument maintenance, malfunction and high variability in particle concentration due to on-site activity.

2.2. Model Formulation

[6] The combined ME2 model extends the traditional chemical mass balance approach by including a simultaneous set of conservation equations for both particle mass and volume, linked by a unique value of apparent particle density for each source

$$x_{ij} = \sum_{k=1}^{p} g_{ik}^{m} f_{kj}^{m} + \varepsilon_{ij} \tag{1}$$

$$v_{iz} = \sum_{k=1}^{p} g_{ik}^{v} f_{kz}^{v} + \varepsilon_{iz}' \tag{2}$$

$$g^{m} = \rho_k g^{v} \tag{3}$$

where for the ith sample, x_{ij} is the jth species concentration ($\mu g/m^3$) and v_{iz} is the volume concentration ($\mu m^3/cm^3$) in the zth size interval, g_{ik}^{m} and g_{ik}^{v} are the particulate mass ($\mu g/m^3$) and volume ($\mu m^3/cm^3$) concentrations from the kth source contributing to the ith sample, f_{kj}^{m} and f_{kz}^{v} are the jth species mass fraction and volume fraction from the kth source, and ρ_k is the average apparent particle density (as opposed to the intrinsic material density [*Bein et al.*, 2005]) of all particles emitted by the kth source.

[7] The size distribution measurements are reported as number concentration (N^p) as a function of size from two different instruments, a differential mobility particle sizer

Table 1. Species Concentrations (ng/m^3; 364 Samples)

Species	Mean	Median	Min	Max	% BDL[a]	R^{2b}
Mass	8300	7100	1900	30100	0	0.96
OC	3100	2650	110	11300	0.3	0.95
EC	650	550	110	2780	9	0.90
Al	11	3	3	122	70	0.26
NH_4^+	490	400	8	3320	0.3	0.99
As	1.1	0.4	0.4	7.4	55	0.36
Br	2.2	1.9	0.4	14.3	8	0.66
Ca	28	24	5	115	0	0.81
Cl	50	6	1.7	1730	42	1.00
Cr	1.6	1.1	0.4	16	29	0.81
Fe	52	42	7	324	0	0.99
Pb	4.2	3.4	1.0	41	16	0.52
Mg	12	5	5	168	77	0.11
Mn	3.3	1.9	0.4	30	24	0.99
Ni	2.6	1.4	0.3	86	24	0.25
NO_3	740	560	120	4820	0	1.00
K^+	30	25	6	200	38	0.73
Si	44	35	3	260	0.3	0.93
Na^+	150	110	14	1120	7	0.94
$SO_4^=$	1260	1140	200	4790	0	0.98
Ta	6.9	2.9	2.9	42	55	0.31
Sn	7.8	3.7	3.7	33	55	0.40
Ti	3.0	2.7	0.7	13	20	0.57
V	3.5	1.9	0.5	47	32	0.99
Zn	9.2	7.2	0.4	48	0.3	0.98

[a]Below method detection limit.
[b]Predicted versus observed (see text).

(DMPS) that provides N^p versus Stokes diameter (d_s) and an aerodynamic particle sizer (APS) that provides N^p versus aerodynamic diameter (d_a). Particle volume can be estimated via:

$$v_{iz} = N_{iz}^p \left(\frac{\pi d_s^3}{6} \right)_z \tag{4}$$

where, for the APS measurements,

$$d_s = {d_a}\Big/{\sqrt{\rho_k}} \tag{5}$$

Note that the apparent particle density not only links g^m to g^v for a given source feature, but also d_s to d_a. In this way, equation (5) acts as an additional constraint on the final solution. This contrasts with the traditional "matching" procedures applied to the size distributions taken with the DMPS and APS where a single apparent particle density is assumed for all particles, rather than a separate density for each source. We have also included the unmeasured mass as another "species." Specifically, the "missing" mass for the *i*th sample is defined as the *m*th species:

$$x_{i,j=m} = (PM_{2.5})_i - \sum_{j=1}^{m-1} x_{ij} \tag{6}$$

where $(PM_{2.5})_i$ is the measured total particle mass concentration for the *i*th sample. Inclusion of the missing mass as an additional variable eliminates the posthoc step of rescaling the results using measured mass, and also provides a useful additional auxiliary equation, specifically for all p sources (k = 1,.p):

$$\sum_{j=1}^{m} f_{kj}^m = 1.0 \pm \delta \tag{7}$$

where δ is a small value, set at 0.01. Given that we measure the entire particle volume at each time period, we can also asserts that for q size intervals

$$\sum_{z=1}^{q} f_{kz}^v = 1.0 \pm \delta \tag{8}$$

We must also require that for each source and for all sizes and species

$$f_k < 1.0 \pm \delta \tag{9}$$

In the absence of sampling artifacts, equations (7)–(9) must be true for all sources, within measurement error.

[8] ME2 provides a solution that minimizes an object function, $Q(E)$, based upon the value of each observation and its corresponding uncertainty. In ME2, the factor analysis problem is solved by using a modified form of the preconditioned Conjugate Gradient algorithm [*Paatero*, 1999]. Also, constraints are imposed in ME2 as in traditional nonnegative least squares (hard constraints). The iteration speed was improved by *Paatero* [1997] adopting a global optimization scheme in which the elements of two matrices vary simultaneously in each iterative step.

[9] Specifically this object function is defined as

$$Q(E) = \sum_{i=1}^{n} \sum_{j=1}^{m} \left[\frac{x_{ij} - \sum_{k=1}^{p} g_{ik}^m f_{kj}^m}{u_{ij}} \right]^2 + \sum_{i=1}^{n} \sum_{z=1}^{q} \left[\frac{\upsilon_{iz} - \sum_{k=1}^{p} g_{ik}^\upsilon f_{kz}^\upsilon}{u_{iz}} \right]^2 \tag{10}$$

where u_{ij} and u_{iz} are the uncertainty estimates in the *j*th species and *z*th size interval measured in the *i*th sample. In

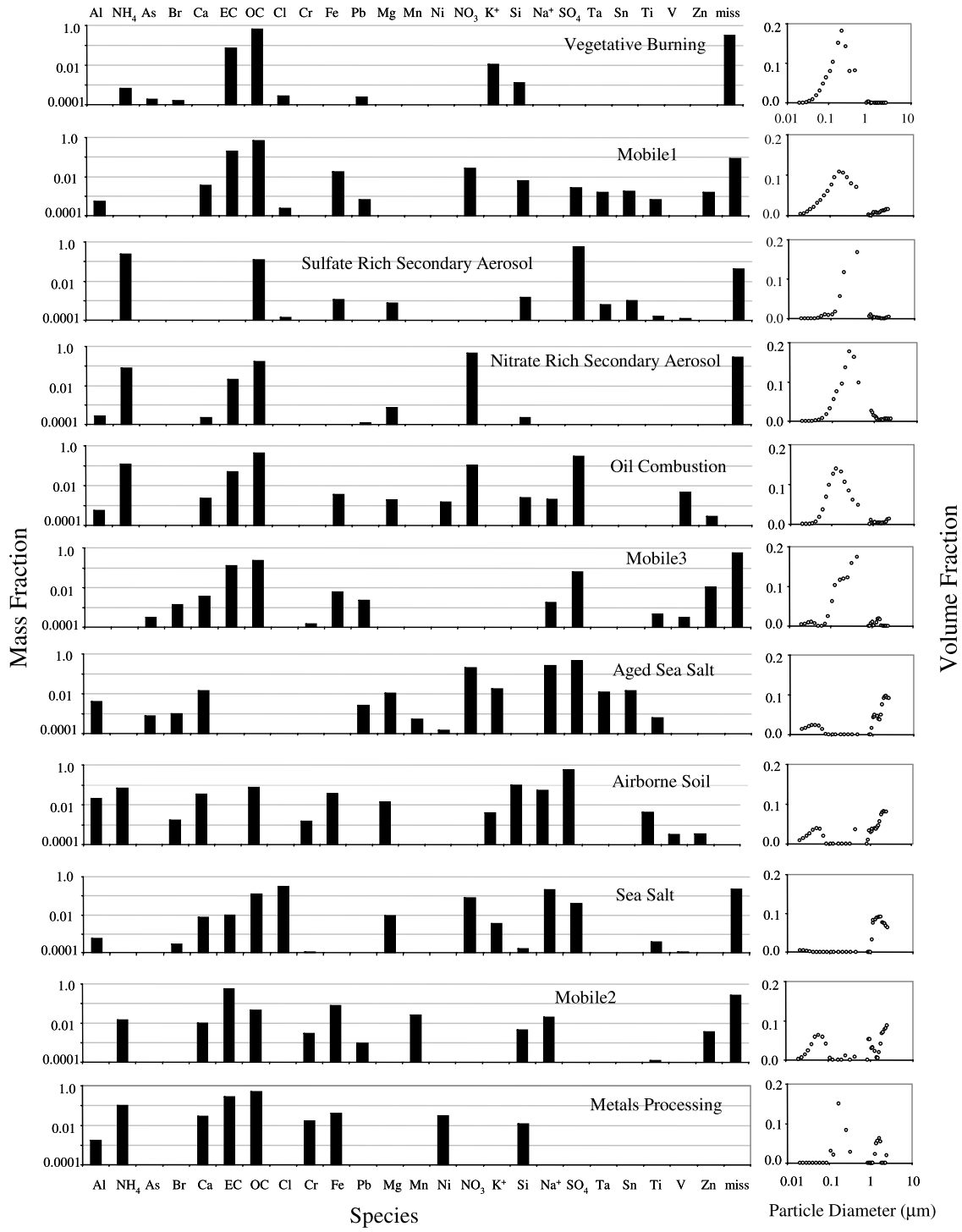

Figure 2. Source profiles including species mass fractions and size distributions (miss, missing particle mass; Stokes diameter for $d_p < 0.5$ μm and aerodynamic diameter for $d_p \geq 0.5$ μm).

addition, ME2 was configured to solve equations (7) and (8) using the auxiliary normalization functions and to set the following hard constraints on the apparent densities:

$$0.7 < \rho_k < 2.5 \tag{11}$$

The constraints described by equations (7), (8) and (11) were solved iteratively by ME2 along with the other governing equations.

2.3. Data Handling

[10] The individual species uncertainties were not available for the STN data. Therefore we estimated the uncertainties using the procedure of Polissar [*Polissar et al.*, 1998, 2001] and the average minimum detection level (MDL) values from Kim and coworkers [*Kim et al.*, 2005]. The measured concentrations below the method detection limit (MDL) values were replaced by half of the MDL values and their uncertainties were set at 5/6 of

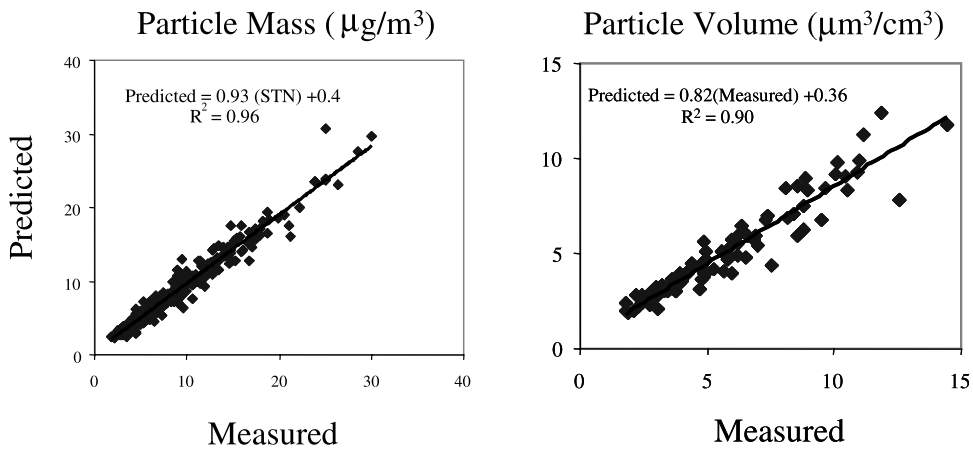

Figure 3. Observed versus predicted particle mass and volume. See text for details on particle volume estimates.

the MDL values. Missing concentrations were replaced by the geometric mean of the concentrations and their accompanying uncertainties were set at four times this geometric mean concentration.

[11] We assigned these estimated uncertainties to each measurement. We then eliminated the following species with more than 80% of their values below the MDL: Sb, Cd, Ce, Cs, Co, Ga, Au, Hf, La, Hg, Nb, P, Rb, Sm, Sc, Tb, W, Y, Eu, In, Ir, Se Mo, Ag and Zr. In addition, we identified Al, As, Mg and Sr as "weak" variables with average measurement to uncertainty ratios < 2, and increased their uncertainties by a factor of 5 [*Paatero and Hopke*, 2003]. We excluded Ba because of a step change in reported concentrations in mid July 2000 resulting in systematically higher values after that time. Cu and Sr were also eliminated for this reason because of similar step changes in April 2002. Because of their greater analytical precision, we also used K^+, Na^+ from ion chromatography rather than K, Na via X-ray fluorescence. In addition, we used sulfate rather than sulfur for purposes of mass closure of $PM_{2.5}$.

[12] To examine the quality of the STN mass measurements we compared the STN values with colocated mass concentrations from the Federal Reference Monitor (FRM). After removing three obvious outliers there was good agreement between the two measures (STN = 0.97 * FRM + 0.1; R^2 = 0.98). To examine the issue of incorrect OC blank values [*Kim et al.*, 2005], we compared the STN mass with that estimated from a mass attribution model [*Malm et al.*, 1994] with a multiplier of 1.4 for OC. There was good agreement between the predicted and measured particle mass concentrations (predicted $PM_{2.5}$ = 0.89 (measured $PM_{2.5}$) + 0.7; R^2 = 0.96). The small but statistically significant intercept is consistent with a small amount of positive OC blank artifact, and the OC data were adjusted downward by this amount. However, any source-related OC sampling artifact is included in the data and therefore the "missing mass" values are lower-limit estimates.

[13] As an additional data screening procedure, we then plotted each species concentration against the measured $PM_{2.5}$ mass concentration in order to look for obvious outliers from an otherwise well defined "edge" associated with a given source feature [*Henry*, 2003]. We eliminated three samples with obvious K^+ outliers and five samples with obvious Si outliers. We also eliminated three samples on 5 July 2000, 3 July 2001, and 4 July 2002 because of possible contributions from fireworks. Our final data set included 24 species, 364 days of chemically speciated data, and 86 days of contemporaneous size distribution data.

[14] The uncertainties of the particle volume measurements were based on the instrument counting statistics [*Kim et al.*, 2004b]. The assumption of constant aerosol

Table 2. Estimated Source Contributions

	Average Contribution, μg/m^3 (Standard Deviation)					
Source Feature	5[a]	10 (Rank Basis)	20	100	∞[b]	Previous Study[c]
Vegetative burning	2.6 (2.5)	2.2 (1.8)	2.2 (1.8)	2.5 (2.3)	2.5 (2.2)	1.4 (1.8)
Mobile 1	0.7 (0.6)	1.4 (1.1)	1.4 (1.2)	0.9 (0.8)	0.9 (0.8)	1.9 (2.0)
Secondary sulfate	1.4 (1.1)	1.2 (1.3)	1.2 (1.0)	1.4 (1.2)	1.4 (1.2)	2.2 (2.0)
Secondary nitrate	1.0 (1.1)	1.2 (1.0)	1.2 (1.3)	1.1 (1.2)	1.1 (1.2)	0.4 (0.4)
Oil combustion	0.4 (0.6)	0.7 (1.1)	0.7 (1.1)	0.4 (0.6)	0.4 (0.7)	0.2 (0.4)
Mobile 3	0.4 (0.3)	0.6 (0.5)	0.6 (0.5)	0.4 (0.3)	0.4 (0.3)	0.8 (1.2)
Aged sea salt	0.7 (0.6)	0.4 (0.3)	0.4 (0.3)	0.4 (0.3)	0.4 (0.3)	0.7 (0.6)
Airborne soil	0.3 (0.2)	0.3 (0.2)	0.3 (0.2)	0.3 (0.3)	0.4 (0.3)	0.6 (0.6)
Sea salt	0.2 (0.5)	0.2 (0.4)	0.1 (0.4)	0.1 (0.4)	0.1 (0.4)	0.3 (0.8)
Mobile 2	0.3 (0.3)	0.1 (0.2)	0.1 (0.1)	0.2 (0.3)	0.3 (0.3)	· · ·
Metals processing	0.3 (0.3)	0.1 (0.06)	0.1 (0.05)	0.2 (0.3)	0.2 (0.3)	0.1 (0.1)

[a]Size distribution down weighting factor (see text).
[b]Size data not included in model; chemical species only.
[c]ME2 analysis of IMPROVE data from 1996 to 2000 [*Kim et al.*, 2004a].

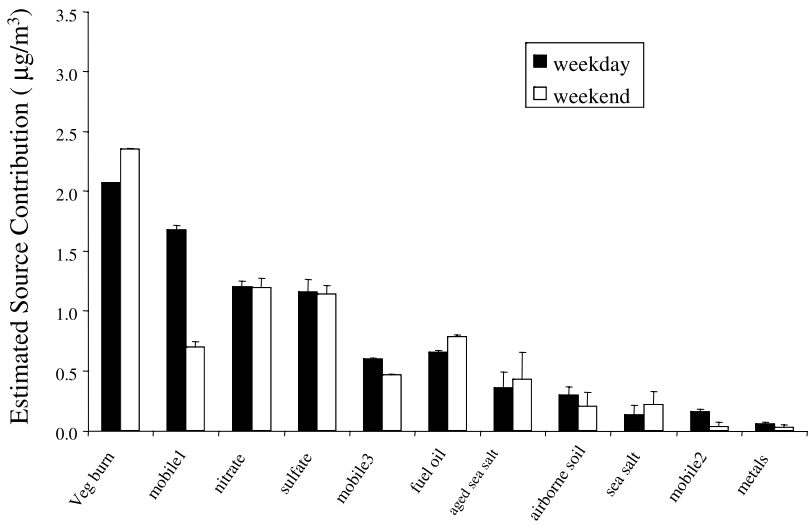

Figure 4. Estimated source contributions ($\mu g/m^3$): Weekday versus weekend.

density versus size is not exact, especially for particle agglomerates such as those emitted from diesel engines [*Shi et al.*, 2000; *Park et al.*, 2004]. This assumption is additionally compounded by the fact that freshly emitted particles can change size and composition during transport from source to receptor because of coagulation, condensation, and chemical reactions such that common sources at different distances would have varying particle densities. Because of the above uncertainties, we chose to consider the size distribution measurements as supplementary to the filter-based species measurements, similar in approach to the use of supplementary meteorological information [*Paatero and Hopke*, 2003]. We therefore down weighted our size distribution measurements by a factor of 10 in order to reduce their importance relative to the chemical measurements.

3. Results

[15] Table 1 summarizes the mass and particulate species concentrations in the final, edited data set. Figure 2 shows the derived source profiles in terms of their mass fraction versus chemical species and their volume fraction versus size, i.e., normalized volume-size distribution. From the constraints imposed by equations (7)–(9), the resulting total mass and volume fractions for each source summed to 1.0 within the specified tolerance of 0.01. Additionally, these constraints produced a direct prediction of the mass fractions and source contributions, avoiding a separate, posthoc rescaling step. An 11-source solution was accepted as the best result, and is also consistent with the previously reported analysis using the species data alone [*Kim et al.*, 2004a]. The 10-source solution did not include the metals profile. The 12-source solution not only produced another small source with negligible mass contribution, but also produced unreasonable apparent source densities: There were three sources with minimum values of 0.7 and three others with maximum values of 2.5.

[16] The predicted versus measured mass and volume concentrations are shown in Figure 3. The "measured volume" concentrations are computed from actual number concentration measurements and an assumption of spherical particles using the Stokes and aerodynamic diameters for the DMPS and APS, respectively. Therefore the predicted

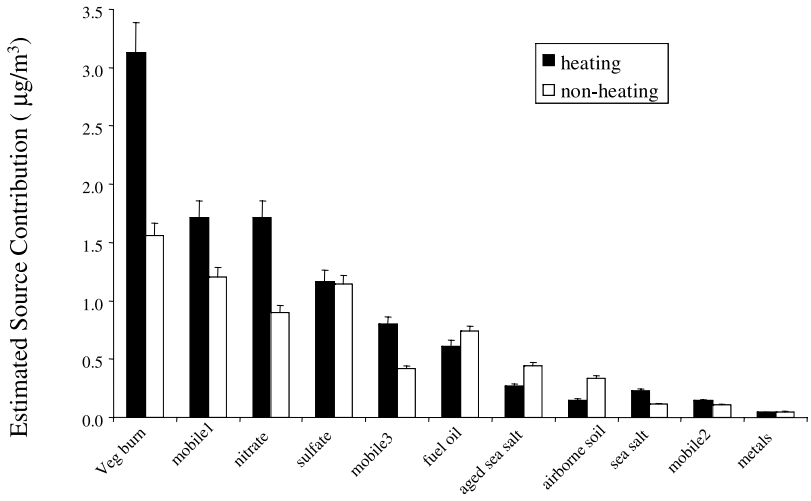

Figure 5. Estimated source contributions ($\mu g/m^3$): Heating versus nonheating seasons.

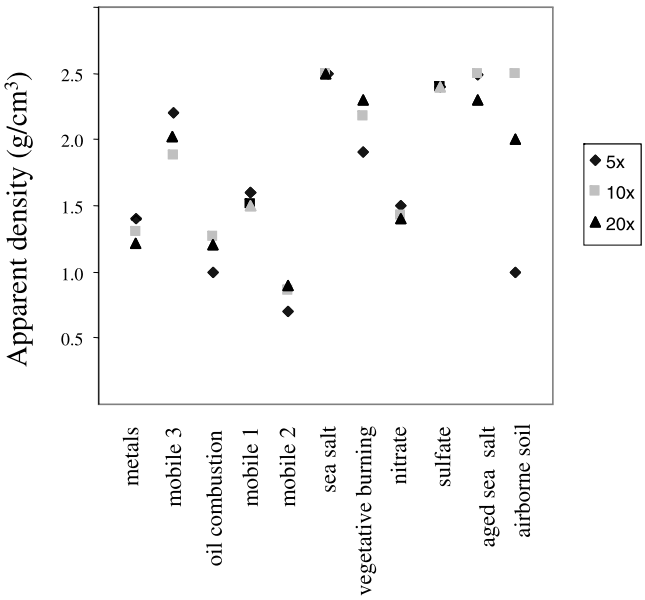

Figure 6. Estimated apparent particle densities by source (g/cm^3). The legend shows the corresponding size distribution down weighting factors (see also Table 2).

"volume" was computed using the predicted mass and apparent density for each source, accounting for the different equivalent diameters as follows:

$$\text{predicted 'volume'} = \sum_{k=1}^{p}\left[\frac{g_k^m}{\rho_k}\left(\sum_{z=1}^{16} f_{kz}^v\right) + g_k^m\sqrt{\rho_k}\left(\sum_{z=17}^{32} f_{kz}^v\right)\right] \tag{12}$$

Table 2 summarizes the average source contributions as a function of the extent of down weighting of the size measurements. (The factor of 10 down weighted results are those presented in Figures 2–5.) There are slight differences as a function of the degree of down weighting, notably between the diesel (i.e., mobile 1 and 2), vegetative burning and aged sea salt estimates. Figure 4 shows the average source contributions separated by weekday versus weekend values. As previously reported [*Lewis et al.*, 2003; *Kim et al.*, 2004a] the average diesel source contribution is significantly higher on weekdays than on weekends. Figure 5 separates the source contributions by heating (October to March) versus nonheating (April to September) season. Again, as expected, the average vegetative burning profile is significantly higher in the heating season. The secondary nitrate feature is also more prominent in the colder, heating season.

[17] Figure 6 shows the apparent particle densities by source for different levels of down weighting of the size measurements. Although these densities vary somewhat as a function of the extent of down weighting, the accompanying source-specific size distributions do not vary much, as shown in Figure 7.

4. Discussion

[18] The measured chemical species concentrations for the data set are given in terms of mean, median, minimum, maximum and percent of total in Table 1. The aerosol was dominated by OC with a mean of 48% of the total mass, followed by sulfate, nitrate, EC, ammonium and sodium at 15, 9, 8, 6, and 2%, respectively. The aggregate of other species accounted for 3% of the measured mass. The missing mass was approximately 10% or less. The concentrations of the species were close to those measured in the four years previous to this study at the IMPROVE site, as reported by *Kim et al.* [2004a].

[19] As shown in Figure 2, the major mass-containing mode varies from ultrafine to accumulation mode to coarse mode depending on the source. The features associated with biomass burning, mobile 1, sulfate, nitrate, oil combustion, mobile 3 and metals processing have volume-size distributions with a single or dominant maximum that occurs in the accumulation mode range, with modal peaks ranging from 0.2 to 0.3 μm diameter. Overall, these secondary aerosol and primary combustion features have predominately fine mode fractions. The vegetative burning profile peaking at about 0.2 μm is consistent with the diluted emissions from wood burning devices [*Kleeman et al.*, 1999]. The peak in secondary nitrate that occurs primarily in the Winter is consistent with preferential partitioning to the condensed phase at lower temperatures [*Wexler and Seinfeld*, 1990; *Clegg et al.*, 1998; *Bein et al.*, 2005; *Tolocka et al.*, 2005].

[20] As expected, the sea salt, aged sea salt, mobile 2 (with resuspended coarse particles) and airborne soil profile size distributions include a substantial volume fraction in the larger size mode. The sea salt feature has a single coarse mode centered about 2 μm. The other features, aged sea salt, airborne soil and mobile 2 have two modes, coarse and ultrafine, that indicate a covariance of one or more species, e.g., coarse soil and ultrafine particles may be resuspended and emitted, respectively, from the same nearby highway. The soil mode is 2.5 μm or larger and undetermined since the upper limit of the useable data from the APS was 2.5 μm. Notably mobile 2 has an ultrafine mode, with a modal diameter of about 0.05 μm. This is larger than the mobile ultrafine mode of ca. 0.03 μm identified in other studies that were sited nearer to mobile sources [*Sardar et al.*, 2005; *Tolocka et al.*, 2005; *Zhang et al.*, 2005].

[21] Our results and those of *Kim et al.* [2004a] are similar in terms of the sources identified as summarized in Table 2. They both show a significant contribution from mobile sources and residual oil combustion at this site, consistent with the fact that it is located not only within 2 km of two major interstate freeways and arterial roads, but also within 4 km of a warehousing area and a major seaport. We identified three different mobile source features whereas Kim only identified two. Our "mobile 1" and "mobile 2" are consistent with "diesel" feature identified in previous apportionment studies at this site [*Maykut et al.*, 2003; *Kim et al.*, 2004a]. They have the highest pair-wise correlation of any two features (r = 0.56). Also, both features have significantly higher contributions on weekdays than on weekends. The "mobile 1" feature is less enriched in EC, Fe and Mn than the "diesel" feature identified in these previous apportionments. However, these same elements are highly enriched in the "mobile 2" feature. From the accompanying size distributions in Figure 2, the "mobile 2" feature is also highly enriched in particles less than 0.1 μm in diameter, is devoid of particles between 0.1 and 1 μm,

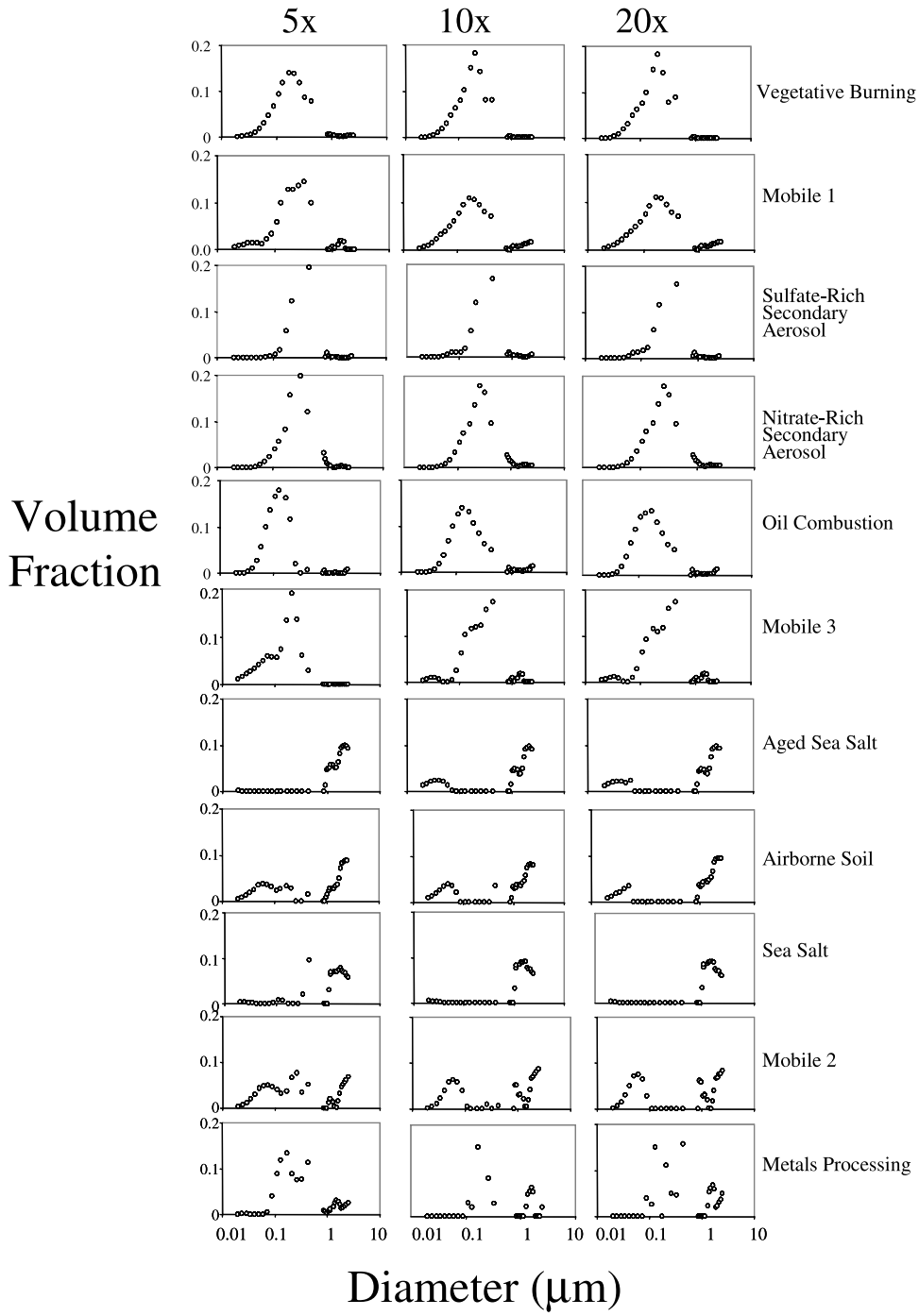

Figure 7. Sensitivity of derived size distributions to the extent of down weighting of the measured values. (See also Table 2 and Figure 6.) Stokes diameter is shown for $d_p < 0.5$ μm and aerodynamic diameter for $d_p \geq 0.5$ μm.

and contains additional coarse material. The significant volume fraction below 0.1 μm is consistent with the size distribution measurements of freshly diluted tailpipe emissions from diesel engines [*Kerminen et al.*, 1997; *Kittelson*, 1998; *Lyyranen et al.*, 1999; *Park et al.*, 2003], vehicle chase studies [*Canagaratna et al.*, 2004] and size-resolved particulate species measurements in heavily trafficked urban areas [*Sardar et al.*, 2005; *Tolocka et al.*, 2005; *Zhang et al.*, 2005]. We therefore interpret these two features as representing diesel sources; "mobile 1" represents the majority of the particle mass from this source in the form of more aged and chemically processed tailpipe emissions from the larger Puget sound region and "mobile 2" represents a minor amount (on a mass basis) of freshly emitted tailpipe emissions combined with some coarse resuspended material which has a short atmospheric lifetime. The separation of the diesel into two source factors resulted from the size information. "Mobile 3" does not show a significant weekday/weekend difference, and is enriched in Zn, similar to the previously identified "gasoline vehicle" feature at

this site [*Maykut et al.*, 2003; *Kim et al.*, 2004a] which is also consistent with the ubiquitous use of the engine anti-wear additive zinc dialkyldithiophospate [*Mosey et al.*, 2005]. This interpretation of these three mobile features is also consistent with the relative source contributions estimates from previous studies (see Table 2).

[22] The overall average apparent particle density was estimated by computing the daily particle volume on the basis of the estimated source mass contributions and the corresponding overall apparent source densities, and plotting this versus the measured daily mass concentration (measured mass [$\mu g/m^3$] = 1.67*daily volume [$\mu m^3/m^3$] + 0.5; R^2 = 0.94). The resulting value of 1.67 ± 0.05 g/cm^3 agrees well with the 23-month average value of 1.6 ± 0.5 g/cm^3 reported by Pitz and coworkers in Erfurt, Germany [*Pitz et al.*, 2003].

[23] The estimated apparent densities fall within the stated bounds, with the exception of the soil, sea salt features and the "mobile 2" feature. The fact that the soil feature has an apparent density above 2.5 and that the freshly emitted diesel feature ("mobile 2") has a value less than 0.7 is not surprising. However, we are cautious not to over interpret these density estimates, given the uncertainties discussed earlier. In order to assign more realistic density constraints, we would need to be able to identify the derived model features a priori (i.e., put priors on the source profiles). It is a natural extension of the model presented here. Even though the derived apparent densities vary somewhat with the extent of down weighting, the source specific size distributions do not (see Figure 7). This is important, given that the main use of these source-specific size distributions is in the interpretation of the species-based features.

5. Conclusions

[24] This study has demonstrated the feasibility of defining missing mass as an additional "species" and of combining daily average volume-size distributions with filter-based species concentrations in a single receptor model of $PM_{2.5}$. The assumption that links these latter two separate data sets is that each contributing source feature at the monitoring site has a constant apparent particle density. Because of this approximation, the size distribution measurements were down weighted by a factor of 10 relative to the filter-based species measurements. Even with this down weighting, the eleven derived source profiles of particle volume versus size were physically reasonable, and the corresponding profiles of species mass fraction as well as the estimated source contributions were consistent with previous studies at this site. The combined model distinguished three mobile source features, two consistent with previous identifications of "gasoline" and "diesel" sources, and an additional minor feature enriched in EC, Fe and Mn and ultrafine particle mass that would have been difficult to interpret in the absence of particle size information.

[25] **Acknowledgments.** This research was supported by the Northwest Research Center for Particulate Air Pollution and Health (U.S. EPA grant CR827355). This study has not been subjected to the U.S. EPA's required peer and policy review. It does not necessarily reflect the views of the U.S. EPA, and no official endorsement should be inferred.

References

Bein, K. J., Y. Zhao, A. S. Wexler, and M. V. Johnston (2005), Speciation of size-resolved individual ultrafine particles in Pittsburgh, Pennsylvania, *J. Geophys. Res.*, *110*, D07S05, doi:10.1029/2004JD004708.

Canagaratna, M. R. J., et al. (2004), Case studies of particulate emissions from in-use New York City vehicles, *Aerosol Sci. Technol.*, *38*, 555–573.

Clegg, S. L., P. Brimblecombe, and A. S. Wexler (1998), Thermodynamic model of the system H+-NH4+SO4 = −NO3−H2O at tropospheric temperatures, *J. Phys. Chem. A*, *102*(12), 2137–2154.

Goswami, E., T. Larson, T. Lumley, and S. L.-J. Liu (2002), Spatial characteristics of fine particulate matter: Identifying representative monitoring locations in Seattle, Washington, *J. Air Waste Manage. Assoc.*, *52*, 324–333.

Henry, R. C. (1997), History and fundamentals of air quality receptor models, *Chemom. Intell. Lab. Syst.*, *37*, 37–42.

Henry, R. C. (2003), Multivariate receptor modeling by N-dimensional edge detection, *Chemom. Intell. Lab. Syst.*, *65*, 179–189.

Hopke, P. K. (1997), Receptor modeling for air quality management, *Environ. Sci. Technol.*, *8*, 95–117.

Kerminen, V. M., T. E. Maleka, C. H. Ojanen, R. E. Hillamo, J. K. Vilhunen, L. Rantanen, N. Havers, A. V. Bohlen, and D. Klockow (1997), Characterization of the particulate phase in the exhaust of a diesel car, *Environ. Sci. Technol.*, *31*, 1883–1889.

Kim, E., P. K. Hopke, T. V. Larson, N. N. Maykut, and J. Lewtas (2004a), Factor analysis of Seattle fine particles, *Aerosol Sci. Technol.*, *38*, 724–738.

Kim, E., P. Hopke, T. V. Larson, and D. S. Covert (2004b), Analysis of ambient particle size distributions using UNMIX and positive matrix factorization, *Environ. Sci. Technol.*, *38*, 202–209.

Kim, E., P. K. Hopke, and Y. Qin (2005), Estimation of organic carbon blank values and error structures of the speciation trends network data for source apportionment, *J. Air Waste Manage. Assoc.*, *55*, 1190–1199.

Kittelson, D. B. (1998), Engines and nanoparticles: A review, *J. Aerosol Sci.*, *29*, 575–588.

Kleeman, M. J., J. J. Schauer, and G. R. Cass (1999), Size and composition distribution of fine particulate matter emitted from wood burning, meat charbroiling, and cigarettes, *Environ. Sci. Technol.*, *33*, 3516–3523.

Lewis, C. W., G. A. Norris, T. L. Conner, and R. C. Henry (2003), Source apportionment of Phoenix PM2.5 aerosol with the Unmix receptor model, *J. Air Waste Manage. Assoc.*, *53*, 325–328.

Lyyranen, J., J. Jokiniemi, E. Kauppinen, and J. Joutsensaari (1999), Aerosol characterisation in medium-speed diesel engines operating with heavy fuel oils, *J. Aerosol Sci.*, *30*, 771–784.

Malm, W. C., J. F. Sisler, D. Huffman, R. A. Eldred, and T. A. Cahill (1994), Spatial and seasonal trends in particle concentration and optical extinction in the United States, *J. Geophys. Res.*, *99*(D1), 1347–1370.

Maykut, N., J. Lewtas, E. Kim, and T. Larson (2003), Source apportionment of PM2.5 at an urban IMPROVE site in Seattle, WA, *Environ. Sci. Technol.*, *37*, 5135–5142.

Mosey, N. J., M. H. Muser, and T. K. Woo (2005), Molecular mechanisms for the functionality of lubricant additives, *Science*, *307*, 1612–1615.

Paatero, P. (1997), Least square formulation of robust non-negative factor analysis, *Chemom. Intell. Lab. Syst.*, *37*, 23–35.

Paatero, P. (1999), The multilinear engine—A table driven, least square program for solving multilinear problems, including the n-way parallel factor analysis model, *Comput. Graphical Stat.*, *8*(4), 854–888.

Paatero, P., and P. K. Hopke (2003), Discarding or downweighting high-noise variables in factor analytic models, *Anal. Chim. Acta*, *490*, 277–289.

Park, K., F. Cao, D. B. Kittleson, and P. H. McMurry (2003), Relationship between particle mass and mobility for diesel exhaust particles, *Environ. Sci. Technol.*, *37*, 577–583.

Park, K., D. B. Kittelson, M. R. Zachariah, and P. H. McMurray (2004), Measurement of inherent material density of nanoparticle agglomerates, *J. Nanopart. Res.*, *6*, 267–272.

Phares, D. J., K. P. Rhoads, M. V. Johnston, and A. S. Wexler (2003), Size-resolved ultrafine particle composition analysis: 2. Houston, *J. Geophys. Res.*, *108*(D7), 8420, doi:10.1029/2001JD001212.

Pitz, M., J. Cyrys, E. Karg, A. Wiedensohler, H. E. Wichmann, and J. Henirich (2003), Variability in apparent particle density of an urban aerosol, *Environ. Sci. Technol.*, *37*, 4336–4342.

Polissar, A. V., P. K. Hopke, P. Paatero, W. C. Malm, and J. F. Sisler (1998), Atmospheric aerosol over Alaska: 1. Elemental composition and sources, *J. Geophys. Res.*, *103*(D15), 19,045–19,057.

Polissar, A. V., P. K. Hopke, and R. L. Poirot (2001), Atmospheric aerosol over Vermont: Chemical composition and source, *Environ. Sci. Technol.*, *35*, 4604–4621.

Research Triangle Institute (2004), Extended semi-annual data summary report for the chemical speciation of PM2.5 filter samples, *Proj. RTI/07565/06DS*, Research Triangle Park, N. C. (Also available as Quality

assurance projects plan chemical speciation of PM2.5 filter samples, Research Triangle Park, N.C. (Available at http://www.epa.gov/ttn/amtic/files/ambient/pm25/spec/rtiqap.pdf)

Rhoads, K. P., D. J. Phares, A. S. Wexler, and M. V. Johnston (2003), Size-resolved ultrafine particle composition analysis: 1. Atlanta, *J. Geophys. Res.*, *108*(D7), 8418, doi:10.1029/2001JD001211.

Ruuskanen, J., et al. (2001), Concentrations of ultrafine, fine and PM2.5 particles in three European cities, *Atmos. Environ.*, *35*(21), 3729–3738.

Sardar, S. B., P. M. Fine, and C. Sioutas (2005), Seasonal and spatial variability of the size-resolved chemical composition of particulate matter (PM_{10}) in the Los Angeles Basin, *J. Geophys. Res.*, *110*, D07S08, doi:10.1029/2004JD004627.

Shi, J. P., D. Mark, and R. M. Harrison (2000), Characterization of particles from a current technology heavy-duty diesel engine, *Environ. Sci. Technol.*, *34*, 748–755.

Tolocka, M. P., D. A. Lake, M. V. Johnston, and A. S. Wexler (2005), Size-resolved fine and ultrafine particle composition in Baltimore, Maryland, *J. Geophys. Res.*, *110*, D07S04, doi:10.1029/2004JD004573.

Wahlin, P., F. Palmgren, R. V. Dingenen, and F. Raes (2001), Experimental studies of ultrafine particles in streets and the relationship to traffic, *Atmos. Environ.*, *35*(S1), S63–S69.

Wexler, A. S., and J. H. Seinfeld (1990), The distribution of ammonium salts among a size and composition dispersed aerosol, *Atmos. Environ., Part A*, *24*, 1231–1246.

Zhang, Q., M. R. Canagaratna, J. T. Jayne, D. R. Worsnop, and J. L. Jimenez (2005), Time- and size-resolved chemical composition of submicron particles in Pittsburgh: Implications for aerosol sources and processes, *J. Geophys. Res.*, *110*, D07S09, doi:10.1029/2004JD004649.

Zhou, L., E. Kim, P. K. Hopke, C. Stanier, and S. N. Pandis (2004), Advanced factor analysis on Pittsburgh particle size distribution data, *Aerosol Sci. Technol.*, *38*, 118–132.

Zhou, L., P. K. Hopke, C. O. Stanier, S. N. Pandis, J. M. Ondov, and P. Pancras (2005), Investigation of the relationship between chemical composition and size distribution of airborne particles by partial least squares and positive matrix factorization, *J. Geophys. Res.*, *110*, D07S18, doi:10.1029/2004JD005050.

D. S. Covert and R. Elleman, Department of Atmospheric Sciences, University of Washington, Seattle, WA 98195, USA.

E. Kim, Department of Civil and Environmental Engineering, Clarkson University, Potsdam, NY 13699, USA.

T. V. Larson, Department of Civil and Environmental Engineering, University of Washington, Seattle, WA 98195, USA. (tlarson@u.washington.edu)

T. Lumley, Department of Biostatistics, University of Washington, Seattle, WA 98195, USA.

A. B. Schreuder, Department of Environmental and Occupational Health Sciences, University of Washington, Seattle, WA 98195, USA.